Biomedical Signal Processing and Control 55 (2020) 101530

Contents lists available at ScienceDirect

Biomedical Signal Processing and Control

journal homepage: www.elsevier.com/locate/bspc

# Computer-aided polyp detection based on image enhancement and saliency-based selection

Farah Deeba*, Francis M. Bui, Khan A. Wahid

*Electrical and Computer Engineering, University of Saskatchewan, Saskatoon, Canada*

ARTICLE INFO

*Article history:*
Received 7 August 2018
Received in revised form 1 April 2019
Accepted 6 April 2019
Available online 17 September 2019

*Keywords:*
Histogram of gradients
Polyp detection
Capsule endoscopy

ABSTRACT

This paper presents a computer-aided polyp detection algorithm applicable to both colonoscopy and wireless capsule endoscopy (WCE). The proposed system has three integral parts: image enhancement, saliency map formation and Histogram of gradients (HOG) feature extraction for final classification. We propose a novel and efficient image enhancement algorithm, which enhances the saliency of clinically important features in endoscopic images. A saliency detection method is applied to the enhanced images to highlight the initial polyp candidates. In the classification stage, polyp candidates are selected after performing an image enhancement step and a saliency detection step. Exhaustive experiments have been performed on three publicly available databases: CVC ColonDB, CVC ClinicDB, and ETIS Larib to evaluate the performance of the proposed polyp detection algorithm. Comparison with the state-of-the-art methods shows that the proposed method outperforms the existing ones in terms of recall (=86.33%) and F2 score (=75.51%) for CVC ColonDB and in terms of recall (=74.04%) for the ETIS Larib dataset. With a significantly reduced number of search windows resulting from the saliency-based selection, the proposed scheme ensures a cost-effective and efficient polyp detection algorithm.



## 1. Introduction

The word 'polyp' is derived from the Greek word 'polyposes', meaning a morbid excrescence. 'Polyp' is an umbrella term encompassing a broad spectrum of lesions, manifested as well-circumscribed tissue mass protruding into the lumen [1]. Polypoid lesions are extremely common in colon and rectum associated with an alarmingly high incidence rate (>30% in the screening colonoscopy) and are precursors to most (>85%) colorectal cancers [2,3]. Early diagnosis and appropriate management of premalignant polyps are crucial to improve the prognosis and survival rate of colorectal cancer.

Colonoscopy is the 'gold standard' method for examining colon and rectum, i.e., large intestine [4]. One downside of the colonoscopic procedure is its low acceptance among the general population [5] due to the invasive nature. For example, the compliance rate to colonoscopy is only 3% per year among the population of Germany, one of the countries with the highest colorectal cancer incidence and mortality [6]. Wireless capsule endoscopy (WCE), a non-invasive and patient-friendly screening technique, is emerging as an alternative diagnostic option. According to the European Society of Gastrointestinal Endoscopy (ESGE) guideline, WCE is recommended for patients with contraindications or patients who are unwilling or unable to undergo conventional colonoscopy [7].

Both colonoscopy and WCE have definitive roles in the diagnosis of polypoid lesions. Nevertheless, screening using both technologies suffers from certain limitations. Manual screening using colonoscopy is associated with a substantial miss rate of polyp [8,9]. Human factors such as "change blindness" and "inattention blindness" are among the factors responsible for the sub-optimum detection rate, which calls for inclusion of a second observer, further adding to the cost [10]. On the other hand, WCE is burdened with the screening of enormous visual information, amounting 14,400-72,000 frames per patient [11]. With the potential to reduce human error and human burden, an automatic computer-aided polyp detection framework can provide diagnostic support for both colonoscopy and WCE procedures. Additionally, widely adopted cancer screening programs are giving rise to a deluge of endoscopic videos, which is a valuable resource for physicians and researchers. Semantic annotation with the aid of automatic image analysis could be useful for realizing the full potential from the available data.

In this paper, we propose a hybrid method combining an image enhancement algorithm and an automated detection system. The proposed automated polyp detector consists of following stages:

* Corresponding author.
*E-mail address:* farah.deeba@usask.ca (F. Deeba).

https://doi.org/10.1016/j.bspc.2019.04.007
1746-8094/

(1) image enhancement, (2) saliency map formation to detect the clinically significant regions, (3) histogram of gradients (HOG) features extraction from the salient regions, and (4) classifier training for final classification. Our contribution can be summarized as follows:

1 To our knowledge, this is the first attempt to combine color enhancement techniques to a computer-aided system. A novel color enhancement method has been proposed to accentuate the minute mucosal detail of the endoscopic images.
2 A computationally efficient implementation of HOG feature based classification has been proposed, by taking into account the most relevant windows.

The rest of the paper is organized as follows: Section 2 highlights the state-of-the-research in the field of polyp detection, Section 3 introduces details of the proposed polyp detection method, and Section 4 presents the detail of experiments, performance evaluation and comparison with the state-of-the-art polyp detection methods. Finally, we conclude the paper with the discussion in Section 5.

## 2. Related works

A substantial amount of research efforts have been invested to develop automated computer-aided detection (CAD) systems for polypoid lesion detection. Among different pathologies targeted in endoscopic frames, polyp detection and classification has remained the most dominant field of research, constituting approximately 47% of all approaches between 1988 to 2010 [12]. A large body of literature can be found for the analysis of colonoscopic, i.e., white light endoscopic (WLE) videos [13–21]. WCE is another area with substantial existing research works [22–28].

The majority of research approaches toward polyp detection are based on the extraction and classification of certain feature descriptors. Polyp detection is a multi-scale detection problem as its size could widely vary depending on actual size variation and relative size variation due to the camera position. The wavelet transform based descriptors, such as color wavelet covariance (CWC) [13], wavelet-based uniform LBP [26,29], wavelet energy feature and wavelet correlation signature [30] have been the basis of a series of research works due to its advantage in the multi-resolution analysis. As an alternative to wavelet transform, curvelet and contourlet transform based textures have been proposed by a few researchers [31,32]. Several studies reveal that combination of color and texture features, compared to color or texture feature alone, is more efficient for the adequate description of polyp [31,15]. Despite being an extensively visited approach, the color-texture feature based methods have been questioned regarding robustness against color and texture variation prevalent in endoscopic videos [33,16].

Recently, shape-based approaches are gaining much attention, where different descriptors are being proposed which can capture the characteristic shape of the polyp. The existing methods have attempted to extract characterizing features of the polyp, such as edge, curvature, protrusion, which make them easily identifiable to the human visual system. In the shape based approaches, shape features are extracted from the ROIs obtained using segmentation contrary to color-texture based approaches where features are extracted from the whole image or fixed shape image patches. Watershed segmentation [14,16], Log Gabor filter [23,25], Hessian filter [34] are examples of the segmentation algorithms adopted in literature. Hwang et al. [14] proposed an elliptical shape based method where shape features like curve direction, curvature, and edge distance of the candidate ellipses were used to detect polyps. The limitation of this attempt to identify polyps with the non-elliptical shape inspired several works with emphasis on more general shape features like edge cross-sectional profile [18] and depth of valleys [16,35]. In addition to shape features, Tajbakhsh et al. [36,33], included context descriptors in the form of image patches around the polyp boundaries. Park et al. [21] proposed a polyp detection framework using eigentissue approach to describe polyp shape and texture.

Finally, diverging from the above-mentioned approaches, a new paradigm is being formed in polyp detection based on popular object recognition, image classification algorithm and deep learning based methods [54]. In the earlier attempts, Histogram of Oriented Gradient (HOG) has been investigated resulting in sub-optimum performance [37,34], and [33]. In a recent study, a variant of HOG (VHOG) in conjunction with Partial Least Square (PLS) method has shown promising results in detecting polyp [20]. HOG feature is robust against noise and illumination change [41] and therefore could be used for characterizing polyp and non-polyp in multimodal images. The main limitations of HOG based method are: (1) the number of patches to be classified could be very large; (2) fixed-size window cannot handle the size variability of the polyps. In this paper, we propose a method to deal with these limitations associated with HOG feature based classification. To reduce the number of patches, we propose a saliency-based selection method to select the initial polyp candidates. HOG features for the positive samples are extracted from the polyp candidates. Additionally, instead of randomly choosing the negative samples out of the enormous possibilities, we select the salient non-polyp regions to train the classifier. Again, only the salient regions enter into the classification stage. This approach significantly reduces the number of windows considered for training and classification and improves computational efficiency.

## 3. The proposed algorithm

An overview of the proposed method has been given in Fig. 1. A detailed description of the steps of the proposed automated polyp detection algorithm is given below.

### 3.1. Image enhancement

A novel image enhancement algorithm is applied to the images to enhance the saliency of the clinically significant regions. The steps of the image enhancement method are detailed in the following sections.

#### 3.1.1. Contrast enhancement

In the contrast enhancement step, the visual appearance of an image is improved by the sharpening of the edge components. In this paper, a linear Unsharp Masking (UM) method has been applied for contrast enhancement. In this method, a scaled high pass filtered version of the image is added to the original image to enhance sharpness along the edges.

Mathematically, the high-pass filtered signal is obtained by subtracting a blurred low-pass filtered version of the image from the original image:

$$I_{highpass}(i) = I(i) - I_{blurred}(i) \quad (1)$$

The low-pass filtered image $I_{blurred}(i)$ is obtained by filtering the original image with a $3 \times 3$ mean filter. Finally, the contrast-enhanced image $I_{enhanced}(i)$ is obtained from the input image I(i) as:

$$I_{enhanced}(i) = I(i) + \lambda \cdot I_{highpass}(i) \quad (2)$$

Here, $I_{highpass}(i)$ is the high-pass filtered version of the input image and $\lambda$ is the scaling factor that determines the degree of contrast enhancement.

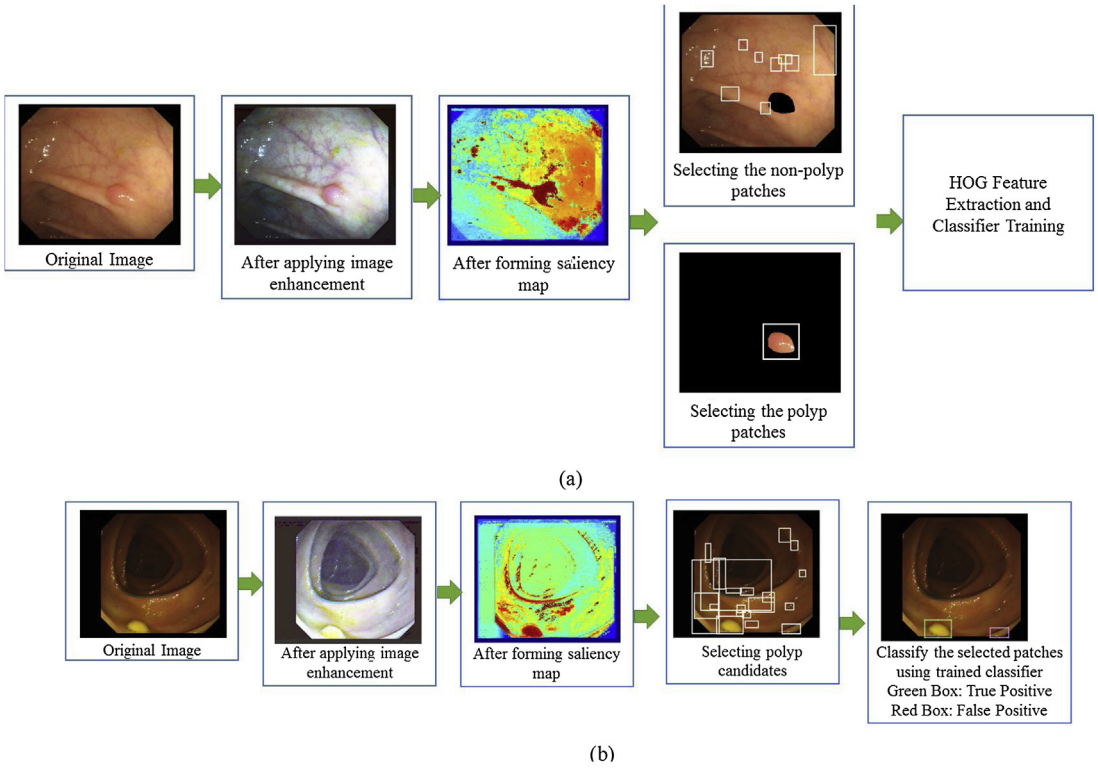


**Fig. 1.** An overview of the proposed polyp detection algorithm. (a) Training Stage; (b) Classification Stage.

#### 3.1.2. Color enhancement

The aim of color enhancement is to enhance the vascular and surface structure of the mucosa in the endoscopic images. Both WLE and WCE typically use full visible wavelength to produce an image. However, light with the specific wavelength is useful to visualize the pattern of certain layers into the mucosa. Short wavelength light, ranging from 400 to 430 nm, has a shallow penetration depth. Therefore, blue light is best-suited to enhance the superficial mucosa structure and to detect the minute mucosal change. Green light, with wavelengths of 525–555 nm, has a deeper penetration depth and corresponds to the second peak of hemoglobin absorption spectra. So, green light is useful for the visualization of thick blood vessels located at the intermediate layer of mucosa (i.e., muscularis mucosa). Therefore, blue and green wavelength light have distinct advantages for the detection of subtle mucosal lesions and inspection of capillary vessels in different layers of mucosa [47].

To capture the image features visible in green and blue light, the endoscopic images are processed accordingly in the color enhancement step. The red component of the endoscopic image is suppressed by a histogram modification technique, where red intensity values are transformed following a modified transform-based gamma correction (TGC) curve:

$$T(i) = (i_{\max} - s)(i/i_{\max})^{\gamma} \tag{3}$$

where $i_{\max}$ is the maximum intensity of the input. The amount of suppression is dictated by both s and γ.

The green and blue components of the endoscopic images are contrast enhanced by utilizing a sigmoidal remapping curve. To enhance the perceived image contrast in the limited dynamic range, both the regions with high intensity and very low intensity have been compressed, whereas the intermediate intensity regions have been stretched [48]. The sigmoidal remapping function is given by:

$$T(i) = i_{\max} \cdot \frac{1}{1 + e^{-a(i-c)}} \tag{4}$$

Here, a and c are coefficients, which were chosen empirically for optimum performance. Based on Eqs. (3) and (4), separate color enhancement curves are formed for red, green and blue color channel (Fig. 2).

### 3.2. Saliency map formation

Motivated by the attention mechanism of the human visual system, the saliency detection algorithm is aimed at capturing the most informative image region without any prior training. The initial success of saliency map formation in differentiating polyp region has been reported [42,49]. In the case of medical images, an abnormality is often displayed as a region with distinctly different intensity distribution compared to that of the surrounding regions. Therefore, the saliency detection algorithm proposed in [50] has been adopted in this paper. The method measures semi-local feature contrast based on a sliding window approach. The saliency of a pixel inside the window is computed by estimating the contrast between inner and outer box. The original image is converted into LUV color space before applying the saliency detection algorithm [42]. Saliency detection algorithms effectively highlight interesting regions including the polyp and polyp-like regions in the endoscopic images.

### 3.3. Feature extraction and classification

While Saliency map highlights the potential polyp candidates, a polyp detector trained using HOG feature is proposed for classifying the candidates as polyp or non-polyp. HOG feature extraction

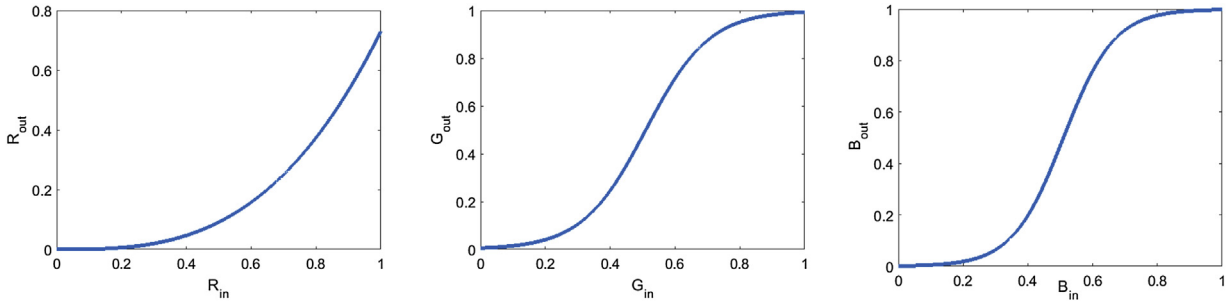


**Fig. 2.** Color enhancement curves for (a) red, (b) green, and (c) blue components of endoscopic images.

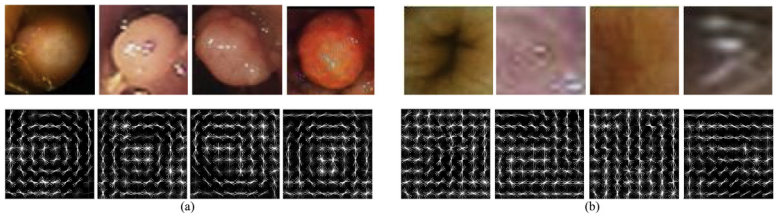


**Fig. 3.** Example of Polyp and non-polyp patches used in training classifier and corresponding HOG feature map. (a) Positive training samples (containing polyp). (b) Negative training samples. Top: endoscopic images; Bottom: extracted HOG feature map from the corresponding image.

method provides a dense overlapping description of image regions by evaluating a dense grid of normalized local histograms of image gradient orientation over the image windows. The underlying assumption is that local gradient can characterize local object appearances, even without the precise knowledge of the corresponding gradient position. The original HOG feature descriptor, as described in [41], contain undirected gradients. Another variant of HOG feature contains both directed and undirected gradients as well as gradient energy features of the neighboring blocks [51]. We extract the variant of HOG features due to its superior performance in discriminating between polyp and non-polyp patches [20]. We also applied principal component analysis (PCA) on the feature space to reduce the feature dimensionality retaining 95% of the variance.

Fig. 3 shows some example positive and negative image patches used in training. The HOG feature maps extracted from the positive patches exhibit dominance of edges creating a similar spherical appearance for different polyps with wide variability in shape, color, and texture. On the other hand, HOG feature maps corresponding to the normal image patches do not exhibit any regular shape and are distinct from those corresponding to polyp patches. In [20], the authors argue that negative samples containing specular reflection, lumen, and mucosal folds have HOG feature appearance similar to polyp patches, causing false positive results. However, in the proposed algorithm, training and test samples are extracted from the visually salient regions. The intermediate step of salient map formation eliminates the majority of negative samples while ensuring the inclusion of all the polyp candidates. The experiments show that most of the patch categories which represent similar HOG features as the polyp, e.g., lumen, mucosal fold, are not visually salient, and therefore do not enter in the classification stage. However, specular reflection is notorious to cause both visually salient and false positive samples with similar HOG feature compared to the polyp. Therefore, specular reflection screening stage is proposed preceded by the classification stage.

In HOG feature based classification, the choice of negative examples and choice of the classifier are two important factors. It is important to include sufficient representative negative examples to improve the generalization capability of the learned classifier, which again introduces imbalance in the training data. In [41], an exhaustive search was performed for false positive (i.e., hard examples) in the training images to limit the number of negative examples, and then linear SVM was applied for classification. On the other hand, data sampling-based boosting framework has been applied to an imbalanced dataset (e.g. polyp to non-polyp patch ratio: 1:1000) where negative examples were randomly selected. Contrary to the previous works, the proposed method applies a saliency-based selection method, resulting in a less imbalanced training dataset (polyp to non-polyp patch ratio: 1:14). For classification, we train linear SVM and RUSBoost classifier [52] and compare their performance.

## 4. Experiments and results

### 4.1. Dataset

A description of the dataset used in our experiments is given in Table 1. All the colonoscopy datasets are provided with the pixel-wise ground truth.

**Table 1**
Description of experimental dataset.

| Database Name | Content | Type | Publicly Available |
|---|---|---|---|
| CVC-ColonDB [16] | 300 polyps in 300 images from 15 different sequences | Colonoscopy | Yes |
| CVC-ClinicDB [35] | 612 polyps in 612 images from 29 different sequences | Colonoscopy | Yes |
| ETIS-Larib [28] | 208 polyps in 196 images | Colonoscopy | Yes |

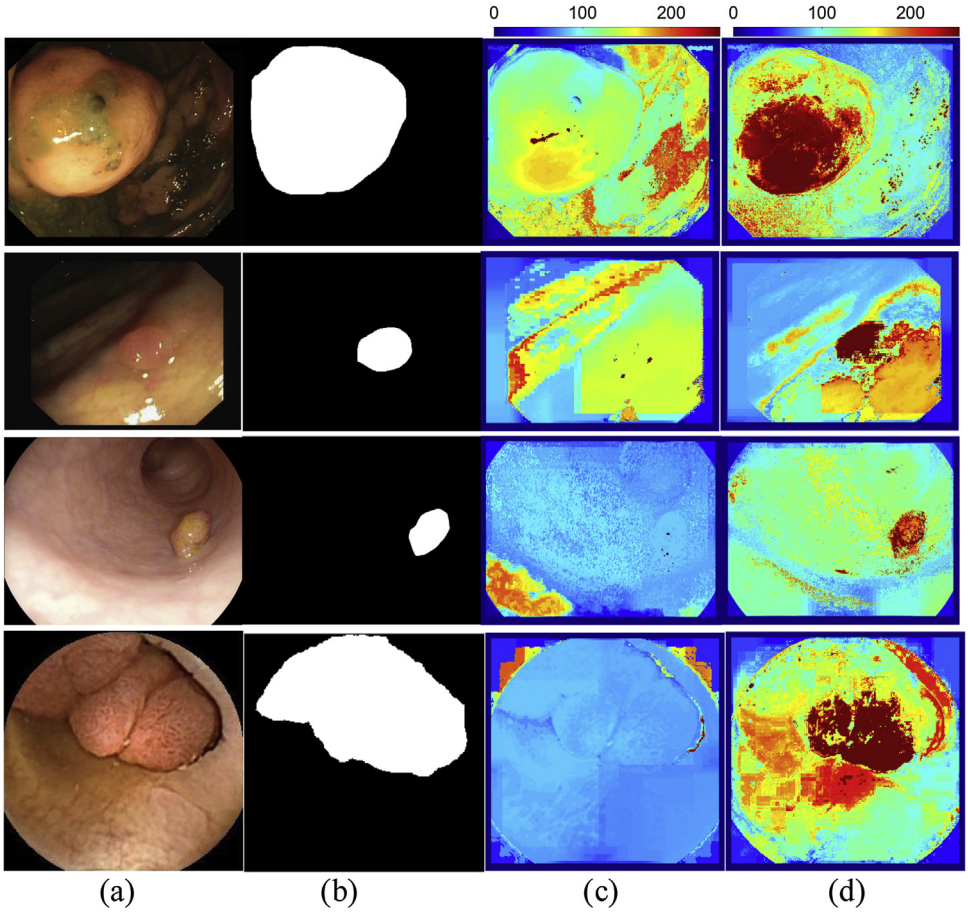


**Fig. 4.** Saliency map for example images are taken from the databases in the order described in Table 1. (a) Example images; (b) Ground truth images; (c) Saliency map obtained without image enhancement; (d) Saliency map obtained after image enhancement.

### 4.2. Implementation

CVC-ClinicDB database has been used for training of the classifiers for all the experiments. CVC-ColonDB and ETIS-Larib databases have been used for testing. For WCE, 800 polyp and 500 non-polyp images have been collected from 20 video clips.

612 positive training samples were extracted by selecting a bounding box surrounding the polyp. As the polyp appearances can be highly variable, the positive training samples are properly scaled and centered to minimize the variance. The image regions in the bounding boxes were cropped and rescaled to $64 \times 64$ pixel image patches. The boundary boxes were selected ensuring that it leaves enough margin around the actual polyp region. On average, 90% of the bounding box area contains the polyp. This measure was taken so that gradients can be computed without any boundary effect.

The negative training samples contain various parts of endoscopic images, except polyp. Rather randomly sampling the image patches to collect the negative samples, image enhancement, and saliency detection steps were performed on the negative images or image parts to find the patches containing clinically important features. After thresholding the saliency map, the salient connected objects in the map are captured by the smallest rectangular shaped bounding boxes which contain the objects. The proposed scheme selects 8328 negative examples from the training images. The regions in the bounding boxes are then cropped and rescaled to $64 \times 64$ pixel image windows. This ensures an intelligent selection of negative examples out of the enormous possibilities and keeps the size of negative training data comparable to the positive samples with minimum information loss.

Then 31- dimensional HOG features were extracted for each cell ($8 \times 8$ pixels) in the training patches. By concatenating the features for $8 \times 8$ cells, 1984- dimensional HOG feature can be extracted for each image patch. The HOG features extracted from both positive and negative training samples are used to train a linear SVM and a RUSBoost classifier. The weak learner used for ensemble learning by RUSBoost is decision tree. The classifiers were optimized and trained using 5-fold cross-validation.

In the testing stage, the test images pass through pre-processing to get rid of the uninformative frames and the image enhancement and saliency map formation steps to select the potential polyp candidates. The saliency map is then thresholded and the salient regions are annotated by rectangular bounding boxes. The annotated regions in the bounding boxes are then cropped, resized to $64 \times 64$ pixels and classified as either polyp or non-polyp using the trained classifiers.

### 4.3. Performance metrics

To evaluate the performance of our proposed method, we measure the following metrics:

$$\text{Precision} = \frac{\text{TP}}{\text{TP+FP}}$$

$$\text{Recall} = \frac{\text{TP}}{\text{TP+FN}}$$

$$\text{F1} = \frac{2 \times \text{Precision} \times \text{Recall}}{\text{Precision + Recall}}$$

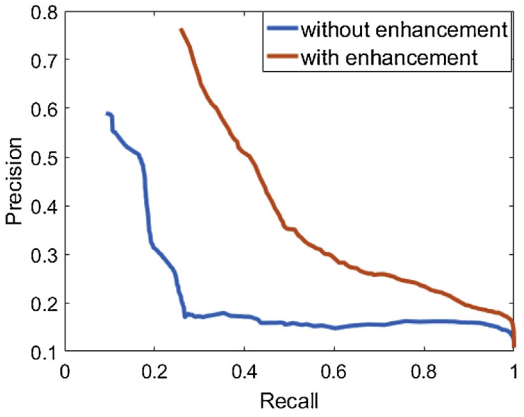


**Fig. 5.** Precision-Recall curve. The blue line and the brown line represent the performance of saliency estimation from images without and with applying image enhancement, respectively.

$$F2 = \frac{5 \times \text{Precision} \times \text{Recall}}{4 \times \text{Precision} + \text{Recall}}$$

A polyp will be considered to be detected if the centroid of the predicted region $F_t$ falls inside the ground truth region. If multiple patches are detected with centroids within the ground truth region, they will be counted as one true positive (TP). A detection patch with centroid that falls outside the ground truth region will be counted as false positive (FP). A false negative (FN) is a polyp that is not detected. Precision computes the percentage of the correct detection among all the detections, whereas recall gives the percentage of the detected polyp among all the polyps.

### 4.4. Saliency detector performance

The efficiency of saliency detection is crucial for the polyp detection framework proposed in this paper. The saliency detection works as the selection method which selects the polyp candidates for final classification. Effective saliency detection is a prerequisite for improved polyp detection performance.

The proposed image enhancement scheme significantly improves the saliency detection performance. Fig. 4 shows a visual comparison of saliency map estimation with and without using the image enhancement method. Application of image enhancement can result in meaningful saliency map formation. To quantitatively estimate the effect of color enhancement on saliency, we calculate pixel-wise recall and precision on a dataset of 150 images. The resulting recall-precision curve has been shown in Fig. 5. From this figure, it is evident that image enhancement significantly improves the saliency detection.

### 4.5. Evaluation on experimental dataset

For evaluating our method, we have taken two publicly available datasets: CVC ColonDB and ETIS-Larib. This allows us to compare our results with those obtained from state-of-the-art algorithms. We apply PCA on the feature space and compare the performance with that before applying PCA using FROC (free-response receiver operating characteristic) analysis. The result has been shown in Fig. 6(a) and (b). The reduced feature set can achieve comparable sensitivity for a fixed FPPI (false positive per image).

As discussed before, our proposed scheme achieves relatively balanced data by means of selection via image enhancement and saliency detection. We compare two classifiers, namely linear SVM and RUSBoost to evaluate the effect of imbalance in training dataset. RUSBoost, a hybrid data sampling and boosting algorithm, is specifically designed to handle class imbalance whereas SVM can lead to a sub-optimum performance in case of highly imbalanced class distribution. From Fig. 6(c), it can be seen that SVM gives an improved result for CVC ColonDB dataset. For ETIS-Larib dataset, no significant difference can be seen between classifier performances.

Tables 2 and 3 detail the result for the selected operating points in our proposed system and the other methods that have recently been suggested in the literature based on CVC ColonDB dataset and ETIS Larib dataset respectively. The tabulated operating points for these systems are selected from Fig. 6. Our proposed method is able to detect the highest number of polyps (259 in CVC ColonDB and 154 in ETIS Larib), outperforming the other state-of-the-art methods by a large margin. Our proposed method has a better trade-off between precision and recall compared to the other methods. In case of CVC ColonDB dataset, our method achieves much higher recall performance, surpassing Bernal et al. [16] and Tajbakhsh [17] by a large margin (about 15% and 23%). For ETIS Larib dataset, our method outperforms CUMED and PLS by about 5% and 17% respectively in terms of recall. Though our method suffers from relatively low precision, it can yield good performance in terms of F1 and F2 score. Low precision implies a burden on the doctors whereas low recall leads to missing of clinically important features preventing the early treatment. Therefore, F1 and F2 score are important performance measures in computer-aided detection systems putting more emphasis on recall than precision. Our method is able to achieve the best F2 score for ETIS-Larib dataset, and comparable F2 score for CVC ColonDB dataset.

## 5. Conclusion and discussion

In this paper, we have proposed an innovative method for polyp detection. The novelty of the method lies in the selection of potential polyp examples using image enhancement and saliency detection. The image enhancement method is an important feature of the algorithm. Table 2 shows that using image enhancement improves the recall value by 50% and precision value by around 20% for CVC ColonDB dataset. Again, an improvement of 37% and 17% can be achieved in recall and precision respectively for ETIS Larib database (Table 3). In the original HOG based human detection algorithm [41], $10^4 - 10^5$ windows have to be tested for a typical image. On the contrary, our saliency-based approach reduces the number of windows to an average of 10.31. This implies a complexity cost reduction by a factor of $10^3$. After selecting potential polyp candidates, we have adopted a simple classification scheme based on HOG feature and RUSBoost or SVM classifier. However, the method can easily be extended to a more sophisticated classification scheme by experimenting on different features and classification method.[1]

Our proposed method is the most similar to the approach proposed in [20]. The recall achieved using our method outperforms [20] with a large margin. We would like to intuitively discuss the reason behind the superior performance of our proposed algorithm. In [20], the negative patches selected for training were taken randomly. During classification, image regions were selected as a sliding window approach from image pyramid with 7 scale levels. It implies that the random selection of training data can miss the hard negative examples which will hamper the optimum training. On the contrary, our algorithm chooses the salient regions in both training and testing phases, thus ensuring the inclusion of most relevant examples and optimum training.

The proposed method is very robust. The performance obtained with and without applying PCA and with different classifiers remain

[1] The results in Table 3 can be found in https://polyp.grand-challenge.org/results/ .

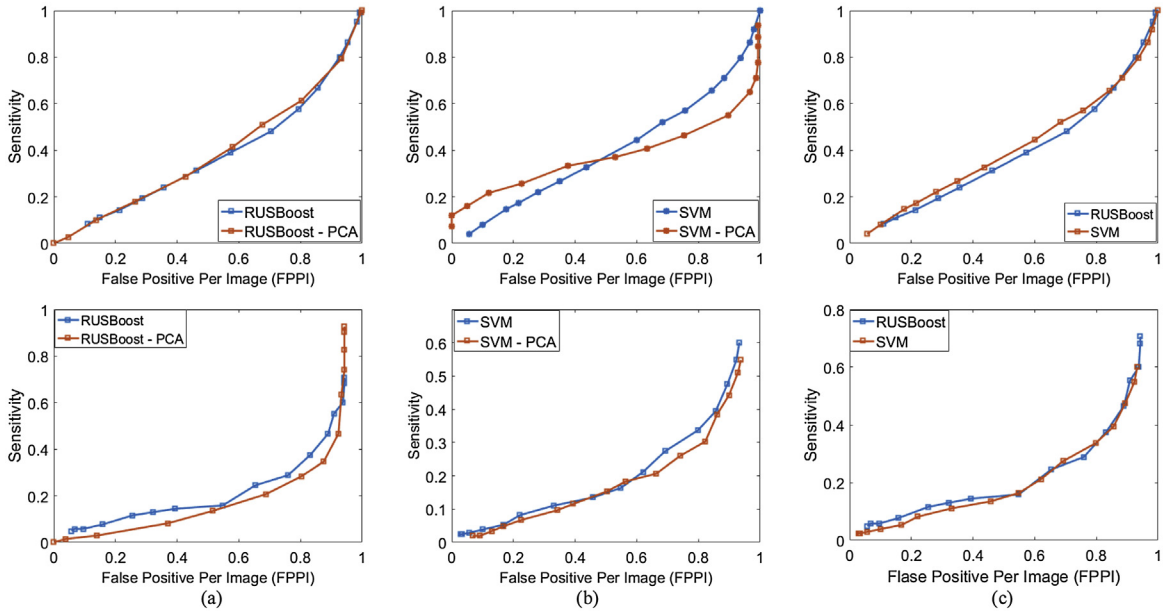


**Fig. 6.** Performance analysis of the proposed method from the FROC curves. Top row: FROC curves evaluated on CVC ColonDB dataset. Bottom row: FROC curves evaluated on ETIS Larib dataset, (a) RUSBoost with and without PCA, (b) SVM with and without PCA, (c) multiple classifiers.

**Table 2**
Comparison of Polyp Detection Performance on CVC ColonDB Dataset.

| Method | Description | TP | FP | FN | Precision | Recall | F1 | F2 |
|---|---|---|---|---|---|---|---|---|
| | Without enhancement | 109 | 253 | 191 | 30.11 | 36.33 | 32.93 | 34.82 |
| | WE-PCA-RB | 238 | 271 | 62 | 46.76 | 79.33 | 58.84 | 69.63 |
| Proposed | WE-RB | 259 | 277 | **41** | 48.32 | **86.33** | 61.96 | 74.60 |
| | WE-PCA-SVM | 254 | 289 | 46 | 46.78 | 84.67 | 60.26 | 72.87 |
| | WE-SVM | **259** | 256 | **41** | 50.29 | **86.33** | 63.56 | **75.51** |
| Bae et al. [20] | Discriminative Feature Learning | 212 | **88** | 88 | 70.67 | 70.67 | 70.67 | 70.67 |
| Bernal et al. [16] | Valley information | 215 | 241 | 85 | 47.15 | 71.67 | 56.88 | 64.92 |
| Bernal et al. [53] | Modified valley information | 203 | 90 | 97 | 69.28 | 67.77 | 68.52 | 68.07 |
| Tajbakhsh [17] | Shape in context | 220 | 90 | 80 | 70.96 | 73.33 | **72.13** | 72.84 |

*WE-with enhancement.

**Table 3**
Comparison of Polyp Detection Performance on ETIS-Larib ColonDB Dataset[1].

| Description | TP | FP | FN | Precision | Recall | F1 | F2 |
|---|---|---|---|---|---|---|---|
| Proposed (Without enhancement) | 76 | 155 | 132 | 32.90 | 36.54 | 34.62 | 35.75 |
| Proposed (WE-PCA-SVM) | 92 | 168 | 116 | 35.38 | 44.23 | 39.31 | 42.12 |
| Proposed (WE- SVM) | 99 | 161 | 109 | 38.08 | 47.60 | 42.31 | 45.33 |
| Proposed (WE-RB) | 115 | 163 | 93 | 41.37 | 55.23 | 47.31 | 51.76 |
| Proposed (WE- PCA-RB) | **154** | 157 | **54** | 49.52 | **74.04** | 51.66 | 67.37 |
| CUMED | 144 | **55** | 64 | 72.36 | 69.23 | **70.76** | **69.83** |
| CVC-CLINIC | 102 | 920 | 106 | 9.98 | 49.04 | 16.58 | 27.51 |
| ETIS-LARIB | 103 | 57 | 77 | 64.375 | 49.52 | 55.98 | 51.92 |
| PLS | 119 | 630 | 89 | 15.89 | 57.21 | 24.87 | 37.64 |
| UNS-UCLAN | 110 | 226 | 98 | 32.74 | 52.88 | 40.44 | 47.09 |

*WE-with enhancement.

similar, as is evident from the FROC analysis (Fig. 6). One limitation of our proposed method is that it suffers from a relatively low precision value. The higher precision in Bae et al. [20] could be attributed to the partial least square analysis based feature learning method. On the other hand, Tajbakhsh [17] uses context information to remove non-polyp structures. In Tajbakhsh [33], a multiclass classification scheme was adopted to learn polyp, vessel, lumen, specular reflection, and random areas. A multi-class classification could be a superior alternative to binary classification to learn the large varieties in non-polyp examples. It should be emphasized that our method can successfully include the relevant regions including polyp and important non-polyp regions in the selection stage while ensuring a balanced and limited data size. However, HOG feature based binary classification is not sufficient to discriminate between some of the hard mimics and polyps. A possible solution is to manually annotate the hard mimics and train a multi-class classifier to generate a more discriminative detector.

To conclude, the proposed polyp detection is fully automated. The detection performance is not sensitive to window size, illumination, and image modality. The method achieves superior polyp detection performance in terms of recall compared to the state-of-the-art methods. In the future, we intend to extend this work by investigating different features, feature selection, and classification scheme. Additionally, multi-class classification can be adopted for

improving precision performance. With the flexibility to include multiple features, the proposed system can be extended to the detection of other abnormalities in endoscopic videos.

## Conflict of interest

We have no conflict of interest to declare.

## Acknowledgements

This work was supported by the Natural Sciences and Engineering Research Council of Canada (NSERC).

## References

[1] Y.P. Do, G.Y. Lauwers, Gastric polyps: classification and management, Arch. Pathol. Lab. Med. 132 (4) (2008) 633–640.
[2] J.H. Bond, Polyp guideline: diagnosis, treatment, and surveillance for patients with nonfamilial colorectal polyps. The practice parameters committee of the American College of Gastroenterology, Ann. Intern. Med. 119 (11) (1993) 836–843.
[3] K. Wallace, et al., Race and prevalence of large bowel polyps among the low-income and uninsured in South Carolina, Dig. Dis. Sci. 61 (1) (2016) 265–272.
[4] N. Shussman, S.D. Wexner, Review Colorectal Polyps and Polyposis Syndromes, 2014, pp. 1–15.
[5] E. Altobelli, A. Lattanzi, R. Paduano, G. Varassi, F. di Orio, Olorectal cancer prevention in Europe: burden of disease and status of screening programs, Prev. Med. (Baltim.) 62 (2014) 132–141.
[6] A. Sieg, K. Friedrich, U. Sieg, Is PillCam COLON capsule endoscopy ready for colorectal cancer screening? A prospective feasibility study in a community gastroenterology practice, Am. J. Gastroenterol. 104 (4) (2009) 848–854.
[7] C. Spada, C. Hassan, et al., Colon capsule endoscopy: European Society of Gastrointestinal Endoscopy (ESGE) Guideline, Endoscopy 44 (5) (2012) 527–536.
[8] T.F. Imperiale, E.A. Glowinski, B.E. Juliar, F. Azzouz, D.F. Ransohoff, Variation in polyp detection rates at screening colonoscopy, Gastrointest. Endosc. 69 (7) (2009) 1288–1295.
[9] A. Gado, B. Ebeid, Gastric cancer missed at endoscopy, Alexandria J. Med. 49 (1) (2013) 25–27.
[10] J. Aranda-Hernández, J. Hwang, G. Kandel, Seeing better – evidence based recommendations on optimizing colonoscopy adenoma detection rate, World J. Gastroenterol. 22 (5) (2016) 1767–1778.
[11] A. Koulaouzidis, E. Rondonotti, A. Karargyris, Small-bowel capsule endoscopy: a ten-point contemporary review, World J. Gastroenterol. 19 (24) (2013) 3726–3746.
[12] M. Liedlgruber, A. Uhl, Computer-aided decision support systems for endoscopy in the gastrointestinal tract: a review, IEEE Rev. Biomed. Eng. 4 (2011) 73–88.
[13] S.A. Karkanis, D.K. Iakovidis, D.E. Maroulis, D.A. Karras, M. Tzivras, Computer-aided tumor detection in endoscopic video using color wavelet features, IEEE Trans. Inf. Technol. Biomed. 7 (3) (2003) 141–152.
[14] S. Hwang, J. Oh, W. Tavanapong, J. Wong, P.C. De Groen, Proc. - Int. Conf. Image Process. ICIP 2 (2007) 465–468.
[15] S. Ameling, S. Wirth, D. Paulus, G. Lacey, F. Vilarino, Texture-based polyp detection in colonoscopy, Bild. für die Medizin 2009 (2009) 346–350.
[16] J. Bernal, J. Sánchez, F. Vilariño, Towards automatic polyp detection with a polyp appearance model, Pattern Recognit. 45 (9) (2012) 3166–3182.
[17] N. Tajbakhsh, S.R. Gurudu, J. Liang, A classification-enhanced vote accumulation scheme for detecting colonic polyps, Lect. Notes Comput. Sci. (including Subser. Lect. Notes Artif. Intell. Lect. Notes Bioinformatics) 8198 LNCS (2013) 53–62.
[18] Y. Wang, W. Tavanapong, J. Wong, J. Oh, P.C. De Groen, Part-based multiderivative edge cross-sectional profiles for polyp detection in colonoscopy, IEEE J. Biomed. Heal. Informatics 18 (4) (2014) 1379–1389.
[19] N. Tajbakhsh, S.R. Gurudu, J. Liang, Automatic polyp detection using global geometric constraints and local intensity variation patterns, Lect. Notes Comput. Sci. (including Subser. Lect. Notes Artif. Intell. Lect. Notes Bioinformatics) 8674 LNCS (PART 2) (2014) 179–187.
[20] S.H. Bae, K.J. Yoon, Polyp detection via imbalanced learning and discriminative feature learning, IEEE Trans. Med. Imaging 34 (11) (2015) 2379–2393.
[21] S.Y. Park, D. Sargent, I. Spofford, K.G. Vosburgh, Y. A-Rahim, A colon video analysis framework for polyp detection, IEEE Trans. Biomed. Eng. 59 (5) (2012) 1408–1418.
[22] L.A. Alexandre, N. Nobre, J. Casteleiro, Color and position versus texture features for endoscopic polyp detection, Biomed. Eng. Informatics New Dev. Futur. - Proc. 1st Int. Conf. Biomed. Eng. Informatics, BMEI 2008 2 (2008) 38–42.
[23] A. Karargyris, N. Bourbakis, Identification of polyps in wireless capsule endoscopy videos using Log gabor filters, in: 2009 IEEE/NIH Life Sci. Syst. Appl. Work. LiSSA 2009, 2009, pp. 143–147.
[24] S. Hwang, Bag-of-visual-words approach to abnormal image detection in wireless capsule endoscopy videos, Lect. Notes Comput. Sci. (including Subser. Lect. Notes Artif. Intell. Lect. Notes Bioinformatics) 6939 LNCS (PART 2) (2011) 320–327.
[25] A. Karargyris, N. Bourbakis, Detection of small bowel polyps and ulcers in wireless capsule endoscopy videos, IEEE Trans. Biomed. Eng. 58 (10 PART 1) (2011) 2777–2786.
[26] B.P. Li, M.Q.H. Meng, Automatic polyp detection for wireless capsule endoscopy images,", Expert Syst. Appl. 39 (12) (2012) 10952–10958.
[27] A.V. Mamonov, I.N. Figueiredo, P.N. Figueiredo, Y.H. Richard Tsai, Automated polyp detection in colon capsule endoscopy, IEEE Trans. Med. Imaging 33 (7) (2014) 1488–1502.
[28] J. Silva, A. Histace, O. Romain, X. Dray, B. Granado, Toward embedded detection of polyps in WCE images for early diagnosis of colorectal cancer, Int. J. Comput. Assist. Radiol. Surg. 9 (2) (2014) 283–293.
[29] B. Li, M.Q.-H. Meng, Tumor recognition in wireless capsule endoscopy images using textural features and SVM-based feature selection, IEEE Trans. Inf. Technol. Biomed. 16 (3) (2012) 323–329.
[30] D.K. Iakovidis, D.E. Maroulis, S.A. Karkanis, An intelligent system for automatic detection of gastrointestinal adenomas in video endoscopy, Comput. Biol. Med. 36 (10) (2006) 1084–1103.
[31] B.P. Li, M.Q.H. Meng, Comparison of several texture features for tumor detection in CE images, J. Med. Syst. 36 (4) (2012) 2463–2469.
[32] Q. Zhao, M.Q.-H. Meng, Polyp detection in wireless capsule endoscopy images using novel color texture features, in: Intell. Control Autom. (WCICA), 2011 9th World Congr., 2011, pp. 948–952.
[33] N. Tajbakhsh, S.R. Gurudu, J. Liang, Automated polyp detection in colonoscopy videos using shape and context information, IEEE Trans. Med. Imaging 35 (2) (2016) 630–644.
[34] Y. Iwahori, T. Shinohara, A. Hattori, R.J. Woodham, S. Fukui, M.K. Behuyan, K. Kasugai, Automatic polyp detection in endoscope images using Hessian filter, Int. Conf. Mach. Vis. Appl. (4) (2013) 21–24.
[35] J. Bernal, et al., WM-DOVA maps for accurate polyp highlighting in colonoscopy: validation vs. saliency maps from physicians, Comput. Med. Imaging Graph. 43 (2015) 99–111.
[36] N. Tajbakhsh, C. Chi, S.R. Gurudu, J. Liang, Automatic polyp detection from learned boundaries, in: 2014 IEEE 11th Int. Symp. Biomed. Imaging, 2014, pp. 97–100.
[37] E. David, R. Boia, A. Malaescu, M. Carnu, Automatic colon polyp detection in endoscopic capsule images, in: ISSCS 2013 - Int. Symp. Signals, Circuits Syst., 2013, pp. 13–16.
[41] N. Dalal, B. Triggs, Histograms of oriented gradients for human detection, in: Proceedings of the IEEE Conference on Computer Vision and Pattern Recognition (CVPR), 2005, pp. 886–893.
[42] F. Deeba, S.K. Mohammed, F.M. Bui, K.A. Wahid, Unsupervised abnormality detection using saliency and retinex based color enhancement, 38th Annu. Int. Conf. IEEE Eng. Med. Biol. Soc. (2016) 3871–3874.
[47] J.Y. Jang, The usefulness of magnifying endoscopy and narrow-band imaging in measuring the depth of invasion before endoscopic submucosal dissection, Clin. Endosc. 45 (4) (2012) 379–385.
[48] G.J. Braun, M.D. Fairchild, Image lightness rescaling using sigmoidal contrast enhancement functions, J. Electron. Imaging 8 (4) (1999) 380.
[49] Y. Yuan, M.Q.H. Meng, Polyp classification based on Bag of Features and saliency in wireless capsule endoscopy, in: 2014 IEEE Int. Conf. Robot. Autom., 2014, pp. 3930–3935.
[50] E. Rahtu, J. Heikkila, A simple and efficient saliency detector for background subtraction, in: 2009 IEEE 12th Int. Conf. Comput. Vis. Work. ICCV Work. 2009, 2009, pp. 1137–1144.
[51] D. Forsyth, Object detection with discriminatively trained part-based models, Computer (Long. Beach. Calif). 47 (2) (2014) 6–7.
[52] C. Seiffert, T.M. Khoshgoftaar, J. Van Hulse, A. Napolitano, RUSBoost: a hybrid approach to alleviating class imbalance.pdf, IEEE Trans. Syst. Man Cybernetics-Part A: Syst. Hum. 40 (1) (2010) 13.
[53] J. Bernal, J. Sanchez, F. Vilarino, Impact of image preprocessing methods on polyp localization in colonoscopy frames, in: 35th Annu. Int. Conf. IEEE EMBS Osaka, Japan, 2013, 2013, pp. 7350–7354, no. c.
[54] Y. Yuan, D. Li, M.Q.H. Meng, Automatic polyp detection via a novel unified bottom-up and top-down saliency approach, IEEE J. Biomed. Health Inform 22 (4) (2018) 1250–1260.